Adhesion of thiolated silica nanoparticles to urinary bladder mucosa: effects of PEGylation, thiol content and particle size

Adhesion of thiolated silica nanoparticles to urinary bladder mucosa: Effects of PEGylation, thiol content and particle size

*Ellina A. Mun, Adrian C. Williams, Vitaliy V. Khutoryanskiy**

Reading School of Pharmacy, University of Reading, Whiteknights, Reading, RG6 6AD, United Kingdom, email: v.khutoryanskiy@reading.ac.uk, Tel: +44(0)1183786119; fax: +44 (0) 118 378 4703

ABSTRACT

Intravesical drug administration is used to deliver cytotoxic agents through a catheter to treat bladder cancer. One major limitation of this approach is poor retention of the drug in the bladder due to periodic urine voiding. Mucoadhesive dosage forms thus offer significant potential to improve drug retention in the bladder. Here, we investigate thiolated silica nanoparticles retention on porcine bladder mucosa *in vitro*, quantified through Wash Out_{50} (WO_{50}) values, defined as the volume of liquid necessary to remove 50% of the adhered particles from a mucosal tissue. Following irrigation with artificial urine solution, the thiolated nanoparticles demonstrate significantly greater retention (WO_{50} up to 36 mL) compared to non-mucoadhesive dextran (WO_{50} 7 mL), but have weaker mucoadhesive properties than chitosan (WO_{50} 89 mL). PEGylation of thiolated silica reduces their mucoadhesion with WO_{50} values of 29 and 8 mL for particles decorated with 750 and 5000 Da PEG, respectively. The retention of thiolated silica nanoparticles is dependent on their thiol group contents and physical dimensions.

KEYWORDS: mucoadhesion, silica nanoparticles, PEGylation, intravesical drug delivery, urinary bladder, thiomers, Wash Out_{50} (WO_{50})

1 INTRODUCTION

Urinary bladder cancer and interstitial cystitis are widespread and serious urological conditions; bladder cancer is the ninth most common cancer in the world, with approximately 430,000 new patients diagnosed with this condition in 2012 (WCRF, 2015). Intravesical drug delivery administers therapeutic agents directly into the urinary bladder via a catheter (Malmstrom, 2003, Gasion and Cruz, 2006, Nirmal et al., 2012, Haupt et al., 2013). This provides localized treatment, minimizes systemic side effects and allows direct exposure of the affected tissue to therapeutic agents. However, intravesical drug delivery also has some limitations. The normal capacity of the bladder is 400–600 mL, but filling to 150–300 mL causes the urge to urinate. Due to periodical voiding of urine from the bladder, instilled drug formulations can be rapidly washed out, requiring frequent repeated administration (Guhasarkar and Banerjee, 2010). Additionally, frequent use of catheters is inconvenient for the patients and may cause inflammatory reactions and infections.

The residence time of a dosage form in the bladder can potentially be improved by using mucoadhesive materials, which could adhere to the epithelial mucosa and resist drug washout. Mucoadhesive formulations for intravesical drug delivery must satisfy three main criteria: they should adhere rapidly to the bladder mucosa, should not

interfere with the normal functions of the bladder and should be retained *in situ* even after urination (Tyagi et al., 2006).

Hydrophilic polymers are traditionally used as mucoadhesive materials in many formulations for transmucosal drug delivery (Peppas, 1996; Andrews, 2009; Khutoryanskiy, 2011) and commonly used are chitosan and carbomers (weakly cross-linked poly(acrylic acid). The adhesion of these polymers to mucosal surfaces is through non-covalent interactions such as hydrogen bonding, electrostatic attraction, hydrophobic effects and diffusion and interpenetration (Khutoryanskiy, 2011). Recently, a number of chemical approaches have been reported to enhance mucoadhesive properties of polymers including the introduction of thiol groups (Bernkop-Schnürch, 2004), acrylate groups (Davidovich-Pinhas, 2011), catechols (Kim, 2015) and boronates (Liu, 2015).

The literature contains few reports on chemically modified and enhanced mucoadhesive materials for intravesical drug delivery. Barthelmes et al (2011, 2013) used thiolated particles based on chitosan and demonstrated that retention in rat bladder *in vivo* was approximately 170-fold greater than for a small-molecular weight fluorescent marker. Storha et al (2013) developed thiolated nanoparticles using thiol-ene click chemistry and studied their retention on porcine urinary bladder mucosa *in vitro*. Zhang et al (2014) reported the synthesis of a series of β-cyclodextrin modified mesoporous silica nanoparticles with hydroxyl, amino, and thiol groups. They demonstrated that retention of thiol-functionalized nanoparticles on the urothelium was significantly higher than the hydroxyl- and amino-functionalized materials.

Previously we have reported the synthesis of thiolated silica nanoparticles using self-condensation of (3-mercaptopropyl)trimethoxysilane in dimethylsulfoxide (Irmukhametova, 2011; Irmukhametova 2012; Mun, 2014a). These nanoparticles

exhibited strong adhesion to ocular tissues and withstood repetitive washes with artificial tear fluid (Irmukhametova, 2011; Mun, 2014b). Here, we evaluate the retention of thiolated and PEGylated silica nanoparticles on porcine urinary bladder *in vitro* and show the effects of nanoparticle size on their mucoadhesive properties. Retention of the nanoparticles depends on both their thiol content and dimensions. Further, we introduce a novel quantitative method to compare the retention efficiency of liquid formulations on mucosal tissues through the use of Wash Out_{50} (WO_{50}) values, defined as the volume of a biological fluid required to wash out 50% of a mucoadhesive formulation from a substrate.

2 MATERIALS AND METHODS

2.1 GENERAL MATERIALS

(3-Mercaptopropyl)-trimethoxysilane (MPTS), dimethyl sulfoxide, dimethyl formamide, acetonitrile, L-cysteine hydrochloride, 5,5'-dithiobis(2-nitrobenzoic acid), 5-(iodoacetamido)-fluorescein, methoxypolyethylene glycol 750 Da maleimide, methoxypolyethylene glycol 5000 Da maleimide, urea, chitosan (103 kDa), fluorescein isothiocyanate (FITC) and fluorescein isothiocyanate dextran (FITC-dextran) were purchased from Sigma-Aldrich (Gillingham, U.K.). Methanol was purchased from Fisher Scientific Ltd (UK) and used as received.

2.2 SYNTHESIS OF THIOLATED SILICA NANOPARTICLES

Thiolated nanoparticles were synthesized according to our previously published protocol (Mun, 2014b). Briefly, 0.75 mL (0.2 mol/L) or 0.38 mL (0.1 mol/L) of MPTS was mixed with 20 mL of DMSO and 0.5 mL of 0.5 mol/L NaOH aqueous solution.

Additionally, the same procedure was repeated with 0.38 mL of MPTS in 20 mL of dimethylformamide (DMF) and acetonitrile. The reaction was conducted with air bubbling and allowed to proceed for 24 hours under constant stirring at room temperature. Nanoparticles were purified by dialysis against deionized water (5L, 8 changes of water) using 12–14 kDa molecular weight cut off dialysis tubing (Medicell International Ltd, UK).

2.3 ELLMAN'S ASSAY

Thiol-group content of the nanoparticles was determined by Ellman's assay. 0.2-0.3 mg of freeze-dried nanoparticles were hydrated in 500 µL of phosphate buffer solution (0.5mol/L, pH 8) and allowed to react with 500 µL of 5,5'-dithio-bis-(2-nitrobenzoic acid) (DTNB) for 2 hours. Absorbance was then measured at 420 nm (Epoch Microplate Spectrophotometer, BioTek Instruments, USA). The calibration curve was constructed with cysteine hydrochloride solutions over the concentration range of 25–175 µmol/L (R^2 = 0.9998).

2.4 SYNTHESIS OF FLUORESCENTLY-LABELLED THIOLATED SILICA NANOPARTICLES

Thiolated silica nanoparticles were labelled with 5-(iodoacetamido)-fluorescein (5-IAF) by adding 3, 0.3, 0.4 and 0.05 mg of 5-IAF to 18, 20, 10 and 10 mL aqueous dispersions of thiolated nanoparticles, respectively. The amount of 5-IAF added was calculated with regard to molar ratios such that 5 µmol of fluorophore was added to 50 µmol of SH-groups of thiolated nanoparticles. The reaction mixture was stirred for 16 hours at room temperature protected from light. Fluorescently-labelled nanoparticles

were then purified by dialysis against deionized water in the dark, according to the above protocol.

2.5 PEGYLATION OF FLUORESCENTLY-LABELLED SILICA NANOPARTICLES

5 mL aqueous dispersions of fluorescently-labelled nanoparticles were mixed with 100 mg of methoxypolyethylene glycol maleimide of two molecular weights (750 or 5000 Da). The reaction mixture was stirred during 16 hours at room temperature protected from light, resulting in the formation of PEGylated silica nanoparticles. PEGylated nanoparticles were purified by dialysis in the dark as above.

2.6 SYNTHESIS OF FLUORESCENTLY-LABELLED CHITOSAN

FITC-chitosan, used as a positive control for mucoadhesion tests, was synthesized according to our previously published protocol (Cook, 2011). 1% w/v chitosan solution was prepared in 100 mL of 0.1 mol/L acetic acid, followed by the addition of 100 mL of dehydrated methanol and 50 mL of 2 mg/mL FITC solution in methanol. The reaction was allowed to proceed for 3 hours in the dark at room temperature and then precipitated in 1 L of 0.1 M NaOH. The precipitate was filtered and dialyzed against 4 L of deionized water in the dark. The resulting product was freeze-dried (Heto Power Dry LL 3000 freeze-drier, Thermo Electron Corporation) and kept wrapped in aluminum foil to avoid exposure to light. For experiments, 0.05% solutions of FITC-chitosan in 0.1 M acetic acid were used.

2.7 PREPARATION OF FLUORESCEIN ISOTHIOCYANATE DEXTRAN (4000 Da) (FITC-DEXTRAN) SOLUTION

FITC-dextran solution, used as a negative control in mucoadhesion studies, was prepared by dissolving 2 mg of FITC-dextran (4000 Da) in 10 mL of deionized water and was left for 5 hours under permanent stirring at room temperature.

2.8 DYNAMIC LIGHT SCATTERING (DLS)

The size of fluorescently-labelled silica nanoparticles and their polydispersity (PDI) values were determined by dynamic light scattering using a Nano-ZS series (Malvern Instruments, UK) at 25°C. Each sample was analyzed three times from which the mean ± standard deviation hydrodynamic diameter values were calculated.

2.9 FLUORESCENCE SPECTROSCOPY

Fluorescence spectra were recorded for fluorescently-labelled thiolated and PEGylated nanoparticles using a FP-6200 Spectrofluorometer (Jasco, UK) over the wavelength range 505–700 nm (λ_{ex}= 492 nm).

2.10 PREPARATION OF ARTIFICIAL URINE SOLUTION

Artificial urine was prepared according to previously published protocol with slight modifications (Chutipongtanate and Thongboonkerd, 2010). The following compounds were dissolved in deionized water by stirring for 3 hours at room temperature, before making the total volume to 2 L: urea (24.27 g), NaCl (6.34 g), KCl (4.50 g), NH_4Cl (1.61 g), $CaCl_2$ (0.67 g), $MgSO_4$•$7H_2O$ (1.00 g), $NaHCO_3$ (0.34 g), Na_2SO_4 (0.26 g), NaH_2PO_4•H_2O (1.00 g), and Na_2HPO_4 (0.11 g). The pH of the resulting solution was 6.2,

which is in agreement with Chutipongtanate and Thongboonkerd (2010). The artificial urine solution was kept at 37° C throughout the experiments.

2.11 MUCOADHESION STUDIES USING PORCINE URINARY BLADDER

Mucoadhesive studies used a fluorescence microscope (Zeiss Imager A1) with an AxioCam MRm Zeiss camera at 5 × magnification with 11.4 ms exposure time and 1388 × 1040 pixels. The porcine urinary bladders used in these experiments were obtained from P.C. Turner Abattoir (Hampshire, UK). Freshly-extracted urinary bladders were transported to the laboratory in a cold box and stored in the fridge at 4°C overnight prior to retention studies. A sample of the bladder tissue (approximately 2 × 3 cm) was carefully excised, avoiding contact with the mucosal side of the tissue, and was briefly rinsed with ~3 mL of artificial urine solution. Experiments were performed with the bladder tissue maintained at 37°C in a water bath. Background microscopy images were recorded for each tissue sample prior to dosing with 200 µL of either fluorescently-labelled nanoparticle dispersion or polymers (controls). Once the test material was placed onto the mucosal surface, fluorescence microscopy images were again taken, followed by 7 washing cycles, for each of which the bladder tissue was irrigated with 10 mL of artificial urine solution at 5 mL/min using a syringe pump. Fluorescence microscopy images (3 for each sample) were recorded initially after treatment and after each wash with the bladder tissue being placed onto a 75 mm x 25 mm glass slide. Each experiment was conducted in triplicate. Microscopy images were analysed with Image J software, the mean fluorescence values (fluorescence, a.u.) after each wash were calculated and a histogram of fluorescence intensity distribution was presented as a function of the volume of artificial urine solution used. The mean fluorescence values were normalized by subtracting the background fluorescence provided by the bladder

189 tissue prior to exposing it to the test material and the initial (pre-wash) fluorescence was
190 taken as an intensity of 1.

191 Since the wash off experiments were not carried out in total darkness, to exclude the
192 possibility of the fluorophore bleaching with time, a portion of thiolated nanoparticles
193 dispersion was placed on the urinary bladder surface and fluorescence measured over
194 5 hours. Figure S1 shows that no significant decrease (Anova, Tukey's multiple
195 comparison's test, p=0.2247) in the fluorescence intensity of nanoparticle dispersion on
196 the bladder surface was observed over 5 hours, indicating their suitability for this type of
197 analysis.

198 WO_{50} values, representing the volume of artificial urine required to wash out 50% of the
199 particles, were calculated from the wash-off profiles. For example, WO_{50} values for
200 chitosan and dextran were calculated via extrapolation of the wash-off results to 50 %
201 using linear and exponential fits, respectively.

202

203

204 # 3 RESULTS AND DISCUSSION

205 ## 3.1 SYNTHESIS AND CHARACTERIZATION OF FLUORESCENTLY-LABELLED
206 THIOLATED AND PEGYLATED SILICA NANOPARTICLES

207 Thiolated silica nanoparticles were synthesized using self-condensation of (3-
208 mercaptopropyl)trimethoxysilane (MPTS) in aprotic solvents in an oxidative environment
209 (bubbling with air) and with small portions of aqueous NaOH as a catalyst. Previously
210 (Mun, 2014b) we showed that the self-condensation of MPTS in dimethylsulfoxide forms
211 nanoparticles of 21±1 nm and 45±1 nm, when the concentration of MPTS in the feed

212 mixture was 0.1mol/L and 0.2 mol/L, respectively. These two types of nanoparticles
213 were also synthesized in the present study. Additionally, in this study we conducted the
214 reaction in other aprotic solvents, namely dimethylformamide (DMF) and acetonitrile
215 (AcN) for nanoparticle synthesis. Maintaining the MPTS at 0.1 mol/L, nanoparticles of
216 95±14 and 217±7 nm were produced in DMF and AcN, respectively. The effect of
217 aprotic solvent nature on the dimensions and properties of thiolated silica nanoparticles
218 has not been reported previously. By changing the concentration of MPTS in the feed
219 mixture and by changing the nature of aprotic solvent it is possible to make the thiolated
220 silica nanoparticles with a range of different sizes. It is widely recognized (Plumere et al,
221 2012) that formation of silica particles from alkoxysilanes (e.g. tetraalkoxysilane)
222 proceeds via several stages such as hydroxysis, condensation, nucleation, aggregation
223 and particle growth. The growth of primary particles as well as their further aggregation
224 are dependent on thermodynamic parameters of the system controlling their colloidal
225 stability. Polarity of the solvent is one of the factors affecting the particles at the
226 nucleation stage. Smaller particles are expected to form in solvents of greater polarity
227 (Wang et al, 2006), which was observed in this work.

228 All nanoparticles were fluorescently labelled by reacting with 5-(iodoacetamido)-
229 fluorescein (5-IAF). The fluorophore was added into the reaction mixture in a 5:50 µmol
230 ratio with regards to the number of SH-groups of silica nanoparticles; thus there were
231 still numerous thiol-groups available for mucoadhesion and for further functionalization.
232 The fluorescently labelled nanoparticles were characterized using dynamic light
233 scattering, fluorescent spectroscopy and Ellman's assay. Figure 1 shows size
234 distributions of the nanoparticles formed in DMSO, DMF and AcN, determined using
235 dynamic light scattering, illustrating the influence of changing solvent polarity on particle
236 size, but with similar dispersities.

Previously (Irmukhametova et al, 2011) it was demonstrated that PEGylation prevents the adhesion of thiolated silica to intact bovine cornea, but could facilitate their penetration into more porous stroma in de-epithelialized cornea (Mun et al, 2014). Clearly, deeper penetration of particles into a biological tissue could also improve their retention, which means that PEGylation may have various effects on particle behavior on different mucosal surfaces. In this work the effect of thiolated silica PEGylation was studied in relation of urinary bladder mucosa.

A portion of fluorescently-labelled thiolated nanoparticles synthesized in DMSO (45±1 nm) was additionally reacted with PEG maleimide of two different molecular weights (750 Da and 5000 Da) to generate two PEGylated silica nanoparticles. The general characteristics of all silica nanoparticles synthesized in this work are summarized in Table 1.

As expected, PEGylation generated larger nanoparticle size distributions, similar to our previous findings (Mun, 2014b). The sizes of thiolated and PEGylated nanoparticles were significantly different (ANOVA; Tukey's multiple comparisons test; $p<0.001$) showing that the greater the molecular weight of PEG shell, the larger the nanoparticles.

PEGylation also reduced thiol groups content from 249±30 µmol/g to 95±6 µmol/g and 78±5 µmol/g, when the nanoparticles were decorated with 750 Da and 5000 Da PEG, respectively. Additionally, due to the screening effect of the PEG shells, reduced fluorescence intensity was observed for PEGylated nanoparticles. PEG of a larger molecular weight provided the lowest fluorescence intensity, since screening with PEG 5000 Da is greater than with PEG 750 Da. For thiolated samples prepared in different solvents, the lowest fluorescence intensity was observed for those synthesized in

acetonitrile, which contained the lowest amount of SH-groups on their surface and hence a lower quantity of the fluorophore conjugated.

3.2 COMPARATIVE MUCOADHESION STUDIES OF THIOLATED AND PEGYLATED NANOPARTICLES

Bernkop-Schnurch introduced thiolated polymers (thiomers) as a new generation of mucoadhesive materials (Bernkop-Schnurch, 2005). Thiomers exhibit enhanced mucoadhesion compared to their unmodified parent polymers due to the formation of disulfide bridges (covalent bonds) between thiol-groups of the polymer and cysteine-rich domains of mucus glycoproteins. Barthelmes et al. (2011) reported the synthesis of chitosan-thioglycolic acid nanoparticles, loaded with trimethoprim, for targeted drug release in the urinary bladder. These nanoparticles enabled controlled and sustainable drug release, showed greater stability and superior mucoadhesion compared to unmodified chitosan particles. The presence of thiol groups on the surface of silica nanoparticles also makes them promising as mucoadhesive materials for application in drug delivery.

The retention of fluorescently-labelled thiolated and PEGylated silica nanoparticles on porcine urinary bladder mucosa was studied using a flow-through method with fluorescent detection (Irmukhametova, 2011; Storha, 2013; Withers, 2013). Figure 2 shows representative fluorescent images of the retention of thiolated and PEGylated silica as well as two controls (chitosan and dextran) on urinary bladder mucosa, washed with artificial urine. Fluorescently-labelled chitosan was selected as a positive control because it is a cationic polymer with well-documented ability to adhere to mucosal

surfaces (Sogias et al., 2008, Khutoryanskiy, 2011). Fluorescently-labelled dextran, on the contrary, had very poor adhesion to mucosal surfaces (Storha, 2013; Withers, 2013), and so was used as a negative control in our experiments.

Analysis of the fluorescent images using ImageJ software allows the retention of fluorescent species on mucosal surfaces to be quantified (Figure 3). FITC-chitosan is retained on the bladder surface even after 7 washes (total volume 70 mL) with artificial urine solution and illustrates its strong interaction with the mucosal surface. However, for FITC-dextran, a significant decrease in fluorescence was observed after the first wash (10 mL) with urine solution, confirming its poor mucoadhesive properties.

Retention of thiolated silica nanoparticles on the bladder mucosa was significantly higher than for FITC-dextran ($p<0.05$): approximately 15% of the fluorescence, hence particles, remains on the mucosal surface even after 7 washing cycles with 10 mL of artificial urine solution. However, their retention was significantly lower than FITC-chitosan ($p<0.05$). This may be due to the polymeric nature of chitosan, whose positively-charged macromolecules are able to penetrate into the mucosal layer of the bladder epithelium, form non-covalent interactions (e.g. electrostatic attraction and hydrogen bonding) with mucins and generate an interpenetration layer (Sogias, 2008). This interpenetration could potentially facilitate better retention of chitosan on the bladder mucosa compared to thiolated nanoparticles.

PEGylated silica nanoparticles were washed from the mucosal surface more rapidly than the thiolated parent particles and hence are less mucoadhesive. The normalized fluorescence intensity of PEGylated (750 Da) nanoparticles on the bladder surface was

similar (T-test, p=0.8937) to that of its thiolated counterpart after the first wash. Whilst the thiolated nanoparticles stayed on the bladder surface after 7 washes, PEGylated (750 Da) nanoparticles were completely removed after 6 washes. PEGylated (5000 Da) nanoparticles revealed poorer retention than when modified with 750 Da PEG and were removed after 5 washes, similar to the negative control, FITC-dextran. Weaker retention for the PEGylated (5000 Da) silica relates to greater screening of the surface thiol groups by the larger molecular weight polymer and to the thiol content on the nanoparticle surface itself (Table 1).

The poorer mucoadhesive performance of PEGylated nanoparticles compared to the thiolated silica is in good agreement with our previous study of retention of similar nanoparticles on the ocular surfaces (Irmukhametova, 2011). However, both thiolated and PEGylated (5000 Da) nanoparticles in our previous report demonstrated a very sharp drop in fluorescence intensity (of 62% and 95%, respectively) after the first wash and the PEGylated nanoparticles were removed from the ocular surface after three washes. Here, PEGylated (PEG 5000 Da) nanoparticles were removed from the bladder mucosa after 6 wash cycles. This discrepancy can be explained by the different nature of two mucosal tissues (Irmukhametova et al., 2011); the rougher structure of the bladder epithelium compared to the cornea provides better retention of silica nanoparticles on its mucosal surface.

Retention studies were conducted with differing sizes of thiolated silica nanoparticles, synthesized in different aprotic solvents (DMSO, DMF and AcN, Table 1). Figure 4 shows the retention profiles for these nanoparticles.

The greatest retention in this series is observed for 21±1 nm thiolated nanoparticles, synthesized in DMSO: they remain on the surface of the bladder mucosa for up to 6-7 washes with 10 mL of artificial urine. The nanoparticles synthesized in DMF are much larger (95±14 nm), but have similar thiol content as the thiolated silica prepared in DMSO (119±12 μmol/g and 118±14 μmol/g, respectively). Their retention on the bladder mucosa is poorer and no traces of these nanoparticles are detectable after 7 wash cycles. This clearly indicates that the nanoparticles of larger size have weaker retention on the bladder mucosa, which is possibly related to their poorer ability to penetrate into the mucosal layer. The weakest retention on the bladder mucosa was observed for the thiolated silica, synthesized in AcN. Both their large size (217±7 nm) and low SH-groups content (40±6 μmol/g) could contribute to this poor mucoadhesive performance.

A comparison between the nanoparticles synthesized in DMSO from the feed mixtures containing different quantities of MPTS reveals that the thiolated silica of 45±1 nm (Figure 3) retains on the bladder mucosa better than 21±1 nm nanoparticles (Figure 4). This is explained by the greater thiol content (249±30 μmol/g) of the 45±1 nm particles compared to 21±1 nm material which had a lower concentration of SH-groups (118±14 μmol/g).

Direct quantitative comparisons between different wash-off profiles is problematic unless each set of data could be converted into a simple numerical value. To this end, we propose WO_{50} values, which represent the volume of a biological fluid required to wash out 50% of the mucoadhesive ingredient from a substrate surface. These values were calculated by analyzing individual wash-off profiles and the results are summarized in Table 1. By comparing these values for different particles used in this study, it is clear that the greatest retention is observed for 45±1 nm thiolated silica particles with the highest SH-groups content (249±30 μmol/g), whose WO_{50} is 36 mL.

PEGylation of these particles reduces their retention with WO_{50} values dropping to 29 and 8 mL for 750 Da and 5000 Da PEG, respectively. Thiolated nanoparticles have greater retention on bladder mucosa compared to non-mucoadhesive dextran (WO_{50} 7 mL), but have weaker mucoadhesive properties than chitosan (WO_{50} 89 mL).

The smallest thiolated particles of 21±1 nm diameter have a lower SH-groups content (118±14 μmol/g) than those of 45±1 nm diameter and showed an expectedly lower WO_{50} of 17 mL. However, the nanoparticles synthesized in DMF are larger (95±14 nm), have a similar SH-groups content (119±12 μmol/g) but are more readily washed from the tissue (WO_{50} 7mL). Hence the retention of particles on mucosal surfaces is not only dependent on their surface thiol-groups but also on their size. Indeed, the largest thiolated particles synthesized in acetonitrile (217±7 nm) have the lowest SH-groups content (40±6 μmol/g) and exhibit weakest retention on mucosal surfaces (WO_{50} = 6 mL).

4.4 CONCLUSIONS

The retention of thiolated and PEGylated silica nanoparticles on porcine urinary bladder mucosa has been studied *in vitro* using fluorescence microscopy. It was shown that the thiolated nanoparticles adhere well to bladder mucosa and withstand wash out effects caused by urine. Retention of these nanoparticles depends on their thiol-content and dimensions. PEGylation of thiolated silica greatly reduces their mucoadhesive properties. The use of WO_{50} values, introduced in this work, provides a convenient method to quantitatively compare the retention of particulates and other materials on differing mucosal surfaces and between differing research protocols.

ACKNOWLEDGEMENTS:

We thank the Leverhulme Trust for funding the *in vitro* retention experiments in this study (RPG-2013-017). EAM is grateful to University of Reading for International Postgraduate Research Studentship. The authors are grateful to P.C. Turner Abattoir (Hampshire, UK) for providing pig bladders for experiments. Dr P. Morrison is acknowledged for the prompt delivery of biological tissues.

REFERENCES:

Andrews G.P., Laverty T.P., Jones D.S. (2009) Mucoadhesive polymeric platforms for controlled drug delivery. European Journal of Pharmaceutics and Biopharmaceutics 71, 505–518

Barthelmes J., Perera G., Hombach J., Dunnhaupt S., Bernkop-Schnurch A. (2011) Development of a mucoadhesive nanoparticulate drug delivery system for a targeted drug release in the bladder. International Journal of Pharmaceutics 416, 339–345

Barthelmes J., Dünnhaupt S., Unterhofer S., Perera G., Schlocker W., Bernkop-Schnürch A. (2013) Thiolated particles as effective intravesical drug delivery systems for treatment of bladder-related diseases. Nanomedicine 8, 65-75.

Bernkop-Schnurch A. (2005) Thiomers: A new generation of mucoadhesive polymers. Advanced Drug Delivery Reviews 57, 1569–1582

405 Chutipongtanate S., Thongboonkerd V. (2010) Systematic comparisons of artificial urine
406 formulas for in vitro cellular study. Analytical Biochemistry 402, 110–112
407
408 Cook M.T., Tzortzis G., Charalampopoulos D. and Khutoryanskiy V.V. (2011)
409 Production and Evaluation of Dry Alginate-Chitosan Microcapsules as an Enteric
410 Delivery Vehicle for Probiotic Bacteria. Biomacromolecules 12, 2834–2840
411
412 Davidovich-Pinhas M. and Bianco-Peled H. (2011) Physical and structural
413 characteristics of acrylated poly(ethylene glycol)-alginate conjugates, Acta Biomaterialia
414 7, 2817-2825.
415
416 Gasion J.P.B., Cruz J.F.J. (2006) Improving efficacy of intravesical chemotherapy.
417 European Urology 50, 225–234
418
419 Guhasarkar S. and Banerjee R. (2010) Intravesical drug delivery: challenges, current
420 status, opportunities and novel strategies. Journal of Controlled Release 148, 147–159
421
422 Haupt M., Thommes M., Heidenreich A., Breitkreutz J (2013) Lipid-based intravesical
423 drug delivery systems with controlled release of trospium chloride for the urinary
424 bladder. Journal of Controlled Release 170, 161–166
425
426 Irmukhametova G.S., Mun G.A., and Khutoryanskiy V.V. (2011) Thiolated
427 mucoadhesive and PEGylated non-mucoadhesive organosilica nanoparticles from 3-
428 mercaptopropyltrimethoxysilane. Langmuir 27, 9551–9556
429

Irmukhametova G.S., Fraser B., Keddie J.L., Mun G.A., Khutoryanskiy V.V. (2012) Hydrogen-Bonding-Driven Self-Assembly of PEGylated Organosilica Nanoparticles with Poly(acrylic acid) in Aqueous Solutions and in Layer-by-Layer Deposition at Solid Surfaces, Langmuir, 28, 299-306

Khutoryanskiy V.V. (2011) Advances in mucoadhesion and mucoadhesive polymers. Macromolecular Bioscience 11, 748–764

Kim K., Kim K., Ryu J.H., Lee H. (2015) Chitosan-catechol: A polymer with long-lasting mucoadhesive properties, Biomaterials 52, 161–170

Liu S., Chang C.N., Verma M.S., Hileeto D., Muntz A., Stahl U., Woods J., Jones L.W., Gu F.X. (2015) Phenylboronic acid modified mucoadhesive nanoparticle drug carriers facilitate weekly treatment of experimentally induced dry eye syndrome. Nano Research 8, 621-635

Malmstrom P-U. (2003) Intravesical therapy of superficial bladder cancer. Critical Reviews in Oncology/Hematology 47, 109–126

Mun E.A., Hannell C., Rogers S.E., Hole P., Williams A.C., Khutoryanskiy V.V. (2014a) On the role of specific interactions in the diffusion of nanoparticles in aqueous polymer solutions, Langmuir, 30, 308-317

Mun E.A., Morrison P.W.J., Williams A.C., Khutoryanskiy V.V. (2014b) On the barrier properties of the cornea: A microscopy study of the penetration of fluorescently labelled nanoparticles, polymers, and sodium fluorescein. Mol. Pharm., 11, 3556-3564

Nirmal J., Chuang Y-C., Tyagi P., Chancellor M.B. (2012) Intravesical therapy for lower urinary tract symptoms. Urological Science 23, 70–77

Peppas N.A. and Sahlin J.J. (1996) Hydrogels as mucoadhesive and bioadhesive materials: a review. Biomaterials 17, 1553–1561

Plumere N., Ruff A., Speiser B., Feldmann, Mayer H.A. (2012) Stober silica particles as basis for redox modifications: Particle shape, size, polydispersity, and porosity. Journal of Colloid and Interface Science, 368, 208-219.

Sogias I.A., Williams A.C., and Khutoryanskiy V.V. (2008) Why is chitosan mucoadhesive? Biomacromolecules 9, 1837–1842

Storha A., Mun E.A. and Khutoryanskiy V.V. (2013) Synthesis of thiolated and acrylated nanoparticles using thiol-ene click chemistry: towards novel mucoadhesive materials for drug delivery. RSC Advances 3, 12275–12279

Tyagi P., Wu P-C., Chancellor M., Yoshimura N., and Huang L. (2006) Recent advances in intravesical drug/gene delivery. Molecular Pharmaceutics 3, 369–379

Wang H.-C., Wu C.-Y., Chung C.-C., Lai M.-H., Chung T.-W. (2006) Analysis of parameters and interaction between parameters in preparation of uniform silicon dioxide nanoparticles using response surface methodology. Industrial and Engineering Chemistry Research 45, 8043-8048

WCRF (2015) http://www.wcrf.org/int/cancer-facts-figures/data-specific-cancers/bladder-cancer-statistics, accessed 17 May 2015

Withers C.A., Cook M.T., Methven L., Gosney M.A., Khutoryanskiy V.V. (2013) Investigation of milk proteins binding to the oral mucosa, Food & Function, 4, 1668–1674

Zhang Q., Neoh K.G., Xu L., Lu S., Kang E.T, Mahendran R., Chiong E. (2014) Functionalized Mesoporous Silica Nanoparticles With Mucoadhesive and Sustained Drug Release Properties for Potential Bladder Cancer Therapy. Langmuir 30, 6151-6161.

Captions to figures

Figure 1. Size distribution of thiolated silica nanoparticles, fluorescently-labelled with 5-IAF

Figure 2. Exemplar fluorescence microphotographs showing retention of FITC-chitosan, thiolated silica, PEGylated silica (750 Da), PEGylated silica (5000 Da) and FITC-dextran on porcine urinary bladder mucosa as washed with different volumes of artificial urine solution. Scale bar is 200 μm.

Figure 3. Fluorescence intensities showing retention of FITC-chitosan, thiolated silica, PEGylated silica (750 Da), PEGylated silica (5000 Da) and FITC-dextran on porcine urinary bladder mucosa after washing with different volumes of artificial urine solution. Each experiment was performed in triplicate and results are presented as the mean value ± standard deviation. Initial intensity after dosing is taken as a value of 1.

Figure 4. Fluorescence levels showing retention of thiolated silica nanoparticles synthesized in DMSO, DMF and AcN on the urinary bladder surface washed with artificial urine. Each experiment was performed in triplicate and the results are presented as the mean value ± standard deviation.

Table 1. Characteristics of fluorescently-labelled thiolated and PEGylated silica nanoparticles

Sample	Diameter, nm	PDI	Nanoparticle concentration, mg/mL	[SH], µmol/g	WO_{50} *, mL
Thiolated (DMSO + 0.2 mol/L MPTS)	45±1	0.332	5	249±30	36
PEGylated (750 Da)	54±1	0.194	5	95±6	29
PEGylated (5000 Da)	69±2	0.145	7	78±5	8
Thiolated (DMSO + 0.1 mol/L MPTS)	21±1	0.263	4	118±14	17
Thiolated (DMF + 0.1 mol/L MPTS)	95±14	0.310	4	119±12	7
Thiolated (AcN+ 0.1 mol/L MPTS)	217±7	0.056	3	40±6	6

* WO_{50} is the volume of artificial urine required to wash out 50% of the particles

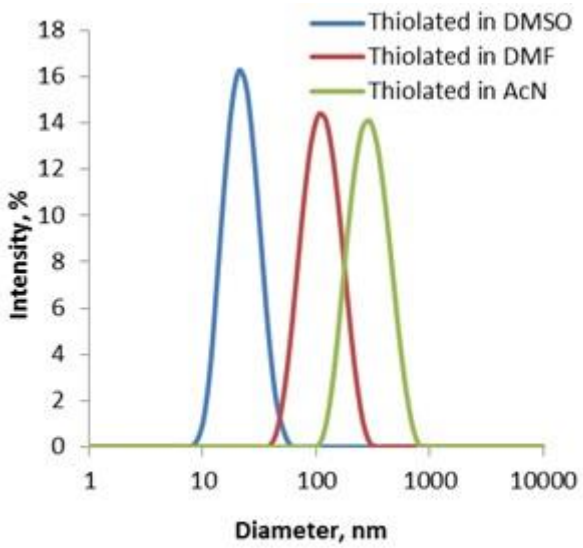

521

522 Figure 1

523

524

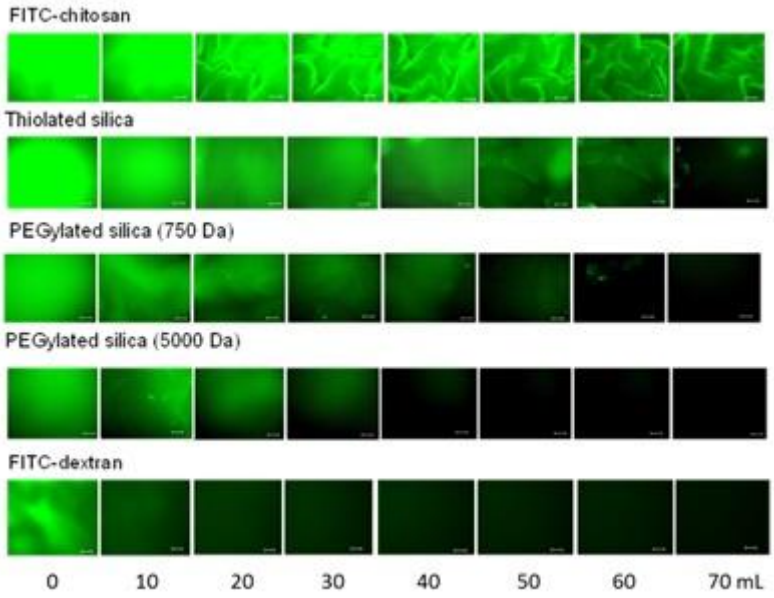

525

526 Figurte 2

527

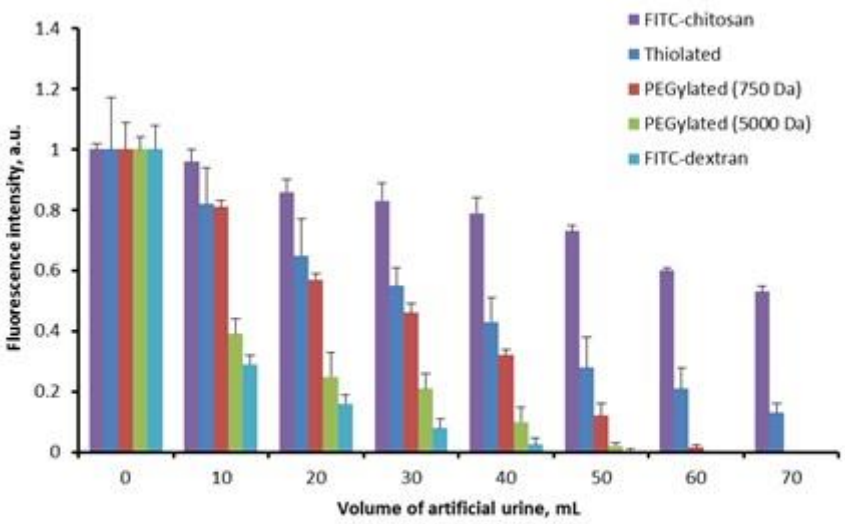

528

529 Figure 3

530

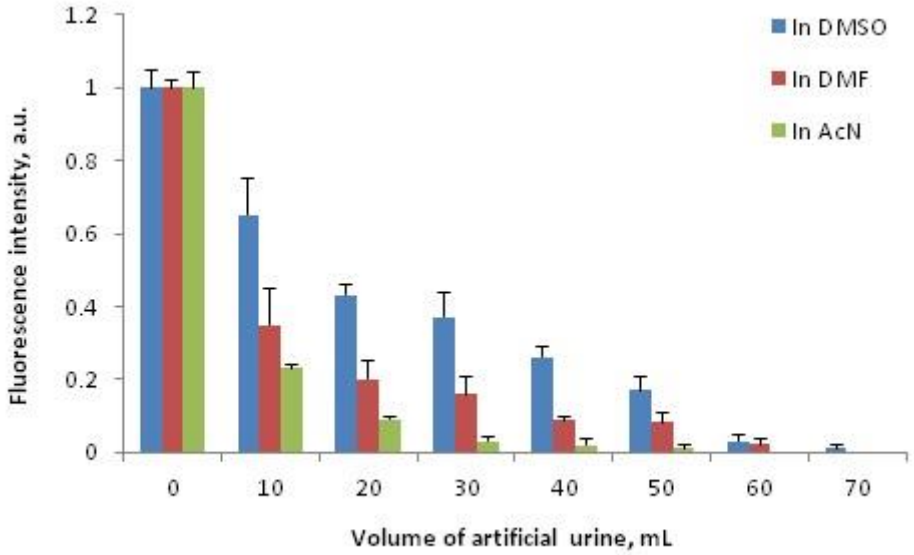

531

532 Figure 4

533

534